

FRACTIONAL MODELLING OF COVID-19 TRANSMISSION INCORPORATING ASYMPTOMATIC AND SUPER-SPREADER INDIVIDUALS

MOEIN KHALIGHI, LEO LAHTI, FAÏÇAL NDAÏROU, PETER RASHKOV,
AND DELFIM F. M. TORRES

ABSTRACT. The COVID-19 pandemic has presented unprecedented challenges worldwide, necessitating effective modelling approaches to understand and control its transmission dynamics. In this study, we propose a novel approach that integrates asymptomatic and super-spreader individuals in a single compartmental model. We highlight the advantages of utilizing incommensurate fractional order derivatives in ordinary differential equations, including increased flexibility in capturing disease dynamics and refined memory effects in the transmission process. We conduct a qualitative analysis of our proposed model, which involves determining the basic reproduction number and analysing the disease-free equilibrium's stability. By fitting the proposed model with real data from Portugal and comparing it with existing models, we demonstrate that the incorporation of supplementary population classes and fractional derivatives significantly improves the model's goodness of fit. Sensitivity analysis further provides valuable insights for designing effective strategies to mitigate the spread of the virus.

1. INTRODUCTION

The worldwide effects of the COVID-19 pandemic have presented challenges to global public health and economies. Refining the understanding of the dynamics of disease transmission can serve in the development of effective strategies for controlling and mitigating the spread of not only COVID-19 but also potential future viral outbreaks. Over the past years, various mathematical models have been developed to describe the spread of the coronavirus SARS-CoV-2, including traditional compartmental models such as SEIR and SIR models [1, 2]. However, these models often assume a homogeneous mixing of individuals and do not fully capture the complex dynamics of the disease, particularly the role of asymptomatic and super-spreader individuals [3].

To overcome these limitations, recent studies have proposed models that incorporate asymptomatic [4, 5] and super-spreader [6, 7] individuals, separately. However, these models may not fully capture the complex interactions between these two types of individuals and their impact on disease transmission dynamics. In our study, we propose a novel

2020 *Mathematics Subject Classification.* Primary: 92D30, 34C60; Secondary: 34A08, 26A33.

Key words and phrases. Mathematical modelling; incommensurate fractional differential equations; COVID-19; asymptomatic individuals; super-spreaders.

approach that integrates both asymptomatic and super-spreader individuals in a single model, taking advantage of fractional calculus to refine the model's performance.

Fractional calculus provides a powerful tool for modelling infectious diseases like COVID-19 due to its ability to incorporate memory and long-range dependence in transmission dynamics [8, 9]. In our study, we utilize incommensurate fractional order derivatives in ordinary differential equations (ODEs) for modelling COVID-19 transmission dynamics, offering two distinct advantages. Firstly, incommensurate fractional order derivatives allow for greater flexibility in capturing the heterogeneous nature of disease dynamics, accounting for factors such as population demographics, social behaviours, and intervention measures that can greatly impact the transmission dynamics [10]. This enables the model to accurately represent the complex and evolving nature of disease spread in real-world scenarios. Secondly, incommensurate fractional order derivatives provide a more refined description of memory effects in the disease transmission process, capturing the long-range dependence and persistence observed in real-world data. This allows for more precise modelling of memory effects, enhancing the accuracy of the model in capturing the impact of past infections on future disease spread.

The structure of the article is as follows. In Section 2, we present some basic definitions and statements from fractional calculus. In Section 3, we introduce our proposed model, which includes different classes of individuals such as susceptible, exposed, symptomatic and infectious, super-spreaders, asymptomatic, hospitalized, recovered, and fatalities. In Section 4, we perform a qualitative analysis of our proposed model, which includes determining the basic reproduction number and analysing the disease-free equilibrium. In Section 5, we present the numerical results, including the fitting of the model with real data from Portugal and a comparison with existing models. We also perform a sensitivity analysis to assess the impact of various model parameters on the basic reproduction number, which provides valuable insights for policy-makers in designing effective strategies to mitigate the spread of emergent infectious diseases. We end with Section 6 of conclusions.

2. BASIC DEFINITIONS AND FUNDAMENTAL PROPERTIES OF FRACTIONAL CALCULUS

We denote the Euclidean norm on \mathbb{R}^n by $\|\cdot\|$.

Definition 2.1. *The Caputo incommensurate fractional derivative of orders $(\alpha_i)_{i=1,\dots,n} \in (0, 1)$ of a function $x : [0, +\infty) \rightarrow \mathbb{R}^n$ is defined by*

$${}^c D^{(\alpha_i)} x(t) = \begin{cases} {}^c D^{\alpha_1} x_1(t), \\ {}^c D^{\alpha_2} x_2(t), \\ \vdots \\ {}^c D^{\alpha_n} x_n(t), \end{cases}$$

with

$${}^c D^{\alpha_i} x_i(t) = \frac{1}{\Gamma(1 - \alpha_i)} \int_0^t (t - s)^{-\alpha_i} x'_i(s) ds,$$

where $\Gamma(1 - \alpha_i) = \int_0^\infty t^{-\alpha_i} \exp(-t) dt$ is the Euler Gamma function.

Note that the value of the Caputo fractional derivative of the function x at time t involves all values of the derivative $x'(s)$ for $s \in [0, t]$, and hence it incorporates the history of x .

We have that ${}^c D^{\alpha_i} x_i(t)$ tends to $x'_i(t)$ as $\alpha_i \rightarrow 1$. In what follows, we recall a fractional Gronwall inequality that is useful to prove existence and uniqueness of the solution to the initial value problem (1).

Lemma 2.2 (Gronwall inequality [11]). *Let α be a positive real number, and let $p(\cdot)$ and $u(\cdot)$ be non-negative continuous functions on $[a, b]$, and $q(\cdot)$ a non-negative, non-decreasing continuous function on $[a, b]$. If*

$$u(t) \leq p(t) + q(t) \int_a^t (t-s)^{\alpha-1} u(s) ds,$$

then

$$u(t) \leq p(t) + \int_a^t \left[\sum_{n=1}^{\infty} \frac{(q(t)\Gamma(\alpha))^n}{\Gamma(n\alpha)} (t-s)^{n\alpha-1} p(s) \right] ds$$

for all $t \in [a, b]$.

Let $f : \mathbb{R}^n \rightarrow \mathbb{R}^n, n > 1$ be a vector field. Consider the following fractional initial value problem:

$$(1) \quad \begin{cases} {}^c D^{(\alpha_i)} x(t) = f(t, x), & \alpha_i \in (0, 1] \\ x(0) = x_0, & x_0 \in \mathbb{R}^n. \end{cases}$$

Theorem 2.3 (Existence and uniqueness of solutions). *Assume that the vector field f satisfies the following conditions:*

- $f(t, x)$ is Lebesgue measurable with respect to t on $[0, +\infty)$;
- $f(t, x)$ and $\frac{\partial f(t, x)}{\partial x}$ are continuous with respect to $x \in \mathbb{R}^n$;
- For two positive constants ω and λ ,

$$(2) \quad \|f(t, x)\| \leq \omega + \lambda \|x\|, \quad \forall x \in \mathbb{R}^n, \quad a.e. t \in [0, +\infty).$$

Then the initial value problem (1) has a unique solution on $[0, +\infty)$.

Proof. The initial value problem (1) can be written in the following vector form:

$$(3) \quad x(t) = x_0 + \int_0^t \text{diag} \left(\frac{(t-s)^{\alpha_i-1}}{\Gamma(\alpha_i)} \right) f(s, x(s)) ds.$$

Let $a, b > 0$ and define the domain

$$\mathcal{D} = \{(t, y) \in [0, +\infty) \times \mathbb{R}^n : t \leq a, \|y - x_0\| \leq b\}.$$

Observe that condition (2) implies that the vector field f is bounded on \mathcal{D} : $\|f(t, x)\| < m, (t, x) \in \mathcal{D}$.

First of all, we must prove the existence and uniqueness of a solution to (1) for $t \in [0, h)$ for some positive $h > 0$.

The idea of the proof follows the ideas of the proof of Theorem 2.1 together with Remark 2.3 of [12]. We show that

$$(4) \quad \text{diag} \left(\frac{(t-s)^{\alpha_i-1}}{\Gamma(\alpha_i)} \right) f(s, \varphi(s))$$

is Lebesgue integrable with respect to $s \in [0, t]$ ($t \leq h \leq a$), provided $\varphi(s)$ is Lebesgue measurable on the interval $[0, h]$. In fact, since the Euler Gamma function is monotone decreasing on $(0, 1]$ and $(t-s)^{\alpha_i-1} < (t-s)^{\alpha_j-1}$ for $\alpha_j < \alpha_i$, we have

$$(5) \quad \int_0^t \left\| \text{diag} \left(\frac{(t-s)^{\alpha_i-1}}{\Gamma(\alpha_i)} \right) f(s, \varphi(s)) ds \right\| \leq \frac{(t-s)^{\alpha_{\min}-1}}{\Gamma(\alpha_{\max})} \|f(s, \varphi(s))\| \leq \frac{(t-s)^{\alpha_{\min}-1}}{\Gamma(\alpha_{\max})} m,$$

where $\alpha_{\min} = \min_{i=1, \dots, n} \alpha_i$, $\alpha_{\max} = \max_{i=1, \dots, n} \alpha_i$. Hölder's inequality implies that (4) is Lebesgue integrable. Using similar estimates, the remainder of the proof follows Steps 2 and 3 from the proof of Theorem 2.1 in [12] to construct a sequence of vector-valued functions $\{\varphi_n(t)\}_{n \in \mathbb{N}}$:

$$\varphi_n(t) = \begin{cases} x_0, & 0 \leq t \leq \frac{h}{n}; \\ x_0 + \int_0^{t-\frac{h}{n}} \text{diag} \left(\frac{(t-s)^{\alpha_i-1}}{\Gamma(\alpha_i)} \right) f(s, x(s)) ds, & \frac{h}{n} \leq t \leq h. \end{cases}$$

Note that in our case we must choose $h < \min\{a, \frac{b\Gamma(\alpha_{\max})\alpha_{\min}}{m}\}$ to construct the sequence of functions $\{\varphi_n(t)\}$.

Following the reasoning in [12], $\varphi_n(t)$ are continuous in $t \in [0, h]$, uniformly bounded, i.e., $(t, \varphi_n(t)) \in \mathcal{D}$, and equicontinuous. These functions can be shown to converge uniformly to a function $\varphi(t)$ on $[0, h]$, which solves (1) on this interval.

Now, it remains to prove that the solution to (1) exists globally. By reduction to absurdity, assume that the solution x admits a maximal existence interval, denoted by $[0, \Pi)$, $\Pi < +\infty$. By substitution of assumption (2) into (3), and applying the relation (5), we get the estimation

$$\|x(t)\| \leq \|x_0\| + \frac{\omega}{\alpha_{\min}\Gamma(\alpha_{\max})} |\Pi|^{\alpha_{\min}} + \frac{\lambda}{\Gamma(\alpha_{\max})} \int_0^t (t-s)^{\alpha_{\min}-1} \|x(s)\| ds.$$

Since λ is a constant, it can be considered a non-negative and non-decreasing function. Thus, by applying the Gronwall inequality of Lemma 2.2, we have that

$$\|x(t)\| \leq K \left(\|x_0\| + \frac{\omega}{\alpha_{\min}\Gamma(\alpha_{\max})} |\Pi|^{\alpha_{\min}} \right),$$

with

$$K = 1 + \int_0^t \sum_{n=1}^{\infty} \frac{\left(\frac{\lambda}{\Gamma(\alpha_{\max})} \Gamma(\alpha_{\min}) \right)^n}{\Gamma(n\alpha_{\min})} (t-s)^{n\alpha_{\min}-1} ds.$$

The rest of the proof follows Theorem 3.1 of reference [12]. □

3. THE MODEL

Transmission of infection from individuals without symptoms is now well documented through the COVID-19 pandemic, see e.g. [13] and references therein. It is also well known that some individuals are super-spreaders, and might transmit the infection to a large number of healthy people [14]. Therefore, it is important to consider these features of transmission by asymptomatic and super-spreader individuals in a single mathematical model. This can be done by enhancing the contact rate between healthy and unhealthy individuals in order to include both routes of infection. Thus, we extend the model in [8] by proposing the following new Caputo incommensurate fractional-order system:

$$(6) \quad \left\{ \begin{array}{l} {}^c D^{\alpha_S} S(t) = -\beta \frac{I}{N} S - l\beta \frac{H}{N} S - \beta' \frac{P}{N} S - \beta'' \frac{A}{N} S, \\ {}^c D^{\alpha_E} E(t) = \beta \frac{I}{N} S + l\beta \frac{H}{N} S + \beta' \frac{P}{N} S + \beta'' \frac{A}{N} S - \kappa E, \\ {}^c D^{\alpha_I} I(t) = \kappa \rho_1 E - (\gamma_a + \gamma_i) I - \delta_i I, \\ {}^c D^{\alpha_P} P(t) = \kappa \rho_2 E - (\gamma_a + \gamma_i) P - \delta_p P, \\ {}^c D^{\alpha_A} A(t) = \kappa(1 - \rho_1 - \rho_2) E - \delta_a A, \\ {}^c D^{\alpha_H} H(t) = \gamma_a(I + P) - \gamma_r H - \delta_h H, \\ {}^c D^{\alpha_R} R(t) = \gamma_i(I + P) + \gamma_r H, \\ {}^c D^{\alpha_F} F(t) = \delta_i I + \delta_p P + \delta_a A + \delta_h H, \end{array} \right.$$

where the fractional orders $\alpha_S, \alpha_E, \alpha_I, \alpha_P, \alpha_A, \alpha_H, \alpha_H, \alpha_F \in (0, 1)$. The model subdivides the human individuals into 8 mutually exclusive classes, namely the susceptible class (S), exposed class (E), symptomatic and infectious class (I), super-spreader class (P), infected but asymptomatic class (A), hospitalized class (H), recovered class (R), and fatality class (F). Here N represents the total population, being given by $N = S + E + I + P + A + H + R + F$.

Susceptible individuals get infected by the virus through a force of infection given by the expression $\beta \frac{I}{N} S + l\beta \frac{H}{N} S + \beta' \frac{P}{N} S + \beta'' \frac{A}{N} S$. This force of infection resembles classical ones, where fewer compartments are used [15].

Notice that P represents super-spreaders among symptomatic individuals only. Super-spreaders among asymptomatic individuals are not differentiated, and their effects are averaged with non-super-spreaders within that group.

Finally, Table 1 presents a comprehensive explanation of the parameters incorporated in our incommensurate Caputo fractional order system (6).

TABLE 1. Description of the parameters used in model (6) and their values.

Parameters	Description	Value	Units
β	Infection rate from infected individuals	fitted	day ⁻¹
β'	Infection rate due to super-spreaders	fitted	day ⁻¹
β''	Infection rate due to asymptomatic individuals	fitted	day ⁻¹
l	Relative transmissibility from hospitalized patients	1.6054	dimensionless
κ	Rate of exposed individuals becoming infectious	0.0366	day ⁻¹
ρ_1	Rate of exposed individuals becoming infected with symptoms	fitted	dimensionless
ρ_2	Rate of exposed individuals becoming super-spreaders	fitted	dimensionless
γ_a	Rate of hospitalization	0.1375	day ⁻¹
γ_i	Recovery rate of non-hospitalized cases	0.0560	day ⁻¹
γ_r	Recovery rate of hospitalized cases	0.9180	day ⁻¹
δ_i	Death rate of infected individuals	0.0442	day ⁻¹
δ_p	Death rate of super-spreaders	fitted	day ⁻¹
δ_h	Death rate of hospitalized individuals	0.0038	day ⁻¹
δ_a	Death rate of asymptomatic individuals	fitted	day ⁻¹

4. QUALITATIVE ANALYSIS

For biological reasons, let us consider the feasible region

$$\Omega = \{(S, E, I, P, A, H, R, F) \in \mathbb{R}_+^8 : S + E + I + P + A + H + R + F \leq N\},$$

together with the initial conditions

$$(7) \quad \begin{aligned} S(0) &\geq 0, \quad E(0) \geq 0, \quad I(0) \geq 0, \quad P(0) \geq 0, \\ A(0) &\geq 0, \quad H(0) \geq 0, \quad R(0) \geq 0, \quad F(0) \geq 0. \end{aligned}$$

The following result holds.

Theorem 4.1. *There exists a unique solution for the initial value problem (6)–(7). Moreover, the solution remains in Ω for all time $t \geq 0$.*

Proof. Let us start by writing the components of the model system (6) as below:

$$(8) \quad X(t) = \begin{pmatrix} S(t) \\ E(t) \\ I(t) \\ P(t) \\ A(t) \\ H(t) \\ R(t) \\ F(t) \end{pmatrix}, \quad F(X) = \begin{pmatrix} -\beta \frac{I}{N} S - l\beta \frac{H}{N} S - \beta' \frac{P}{N} S - \beta'' \frac{A}{N} S \\ \beta \frac{I}{N} S + l\beta \frac{H}{N} S + \beta' \frac{P}{N} S + \beta'' \frac{A}{N} S - \kappa E \\ \kappa \rho_1 E - (\gamma_a + \gamma_i) I - \delta_i I \\ \kappa \rho_2 E - (\gamma_a + \gamma_i) P - \delta_p P \\ \kappa(1 - \rho_1 - \rho_2) E - \delta_a A \\ \gamma_a(I + P) - \gamma_r H - \delta_h H \\ \gamma_i(I + P) + \gamma_r H \\ \delta_i I + \delta_p P + \delta_a A + \delta_h H \end{pmatrix}.$$

It is not hard to check that the vector field F satisfies the first condition of Theorem 2.3. It remains only to show the second condition. For this purpose, set

$$A_1 = \begin{pmatrix} 0 & 0 & -\beta & -\beta' & -\beta'' & -l\beta & 0 & 0 \\ 0 & 0 & \beta & \beta' & \beta'' & l\beta & 0 & 0 \\ 0 & 0 & 0 & 0 & 0 & 0 & 0 & 0 \\ 0 & 0 & 0 & 0 & 0 & 0 & 0 & 0 \\ 0 & 0 & 0 & 0 & 0 & 0 & 0 & 0 \\ 0 & 0 & 0 & 0 & 0 & 0 & 0 & 0 \\ 0 & 0 & 0 & 0 & 0 & 0 & 0 & 0 \\ 0 & 0 & 0 & 0 & 0 & 0 & 0 & 0 \end{pmatrix}, \quad A_2 = \begin{pmatrix} 0 & 0 & 0 & 0 & 0 & 0 & 0 & 0 \\ 0 & -\kappa & 0 & 0 & 0 & 0 & 0 & 0 \\ 0 & \kappa\rho_1 & -\varpi_i & 0 & 0 & 0 & 0 & 0 \\ 0 & \kappa\rho_2 & 0 & -\varpi_p & 0 & 0 & 0 & 0 \\ 0 & \varpi_e & 0 & 0 & -\delta_a & 0 & 0 & 0 \\ 0 & 0 & \gamma_a & \gamma_a & 0 & -\varpi_h & 0 & 0 \\ 0 & 0 & \gamma_i & \gamma_i & 0 & \gamma_r & 0 & 0 \\ 0 & 0 & \delta_i & \delta_p & \delta_a & \delta_h & 0 & 0 \end{pmatrix},$$

with $\varpi_e = \kappa(1 - \rho_1 - \rho_2)$; $\varpi_i = \gamma_a + \gamma_i + \delta_i$; $\varpi_p = \gamma_a + \gamma_i + \delta_p$ and $\varpi_h = \gamma_r + \delta_h$. Therefore, F can be expanded as $F(X) = \frac{S}{N}A_1X + A_2X$, and this leads to

$$\|F(X)\| \leq \|A_1X\| + \|A_2X\| < \epsilon + (A_1 + A_2)\|X\|,$$

for any positive constant ϵ . Hence, it follows from Theorem 2.3 that the model system (6) subject to (7) has a unique solution. \square

It is of great importance to determine the basic reproduction number \mathcal{R}_0 for the epidemiological model (6). This quantity represents the number of cases one infected case generates on average throughout the infectious period, in an otherwise fully susceptible population. Following [6, 7], we prove the following theorem.

Theorem 4.2. *The basic reproduction number associated to the model system (6) is*

$$(9) \quad \mathcal{R}_0 = \frac{\beta\rho_1(\gamma_a l + \varpi_h)}{\varpi_h \varpi_i} + \frac{\rho_2(\beta\gamma_a l + \beta' \varpi_h)}{\varpi_h \varpi_p} + \frac{\beta''(1 - \rho_1 - \rho_2)}{\delta_a}.$$

Proof. The proof is done by the well-known next generation matrix approach [16] applied to our model. For this, the following next generation matrices hold:

$$F = \begin{pmatrix} 0 & \beta & \beta' & \beta'' & l\beta \\ 0 & 0 & 0 & 0 & 0 \\ 0 & 0 & 0 & 0 & 0 \\ 0 & 0 & 0 & 0 & 0 \\ 0 & 0 & 0 & 0 & 0 \end{pmatrix}, \quad V = \begin{pmatrix} \kappa & 0 & 0 & 0 & 0 \\ -\kappa\rho_1 & \varpi_i & 0 & 0 & 0 \\ -\kappa\rho_2 & 0 & \varpi_p & 0 & 0 \\ -\varpi_e & 0 & 0 & \delta_a & 0 \\ 0 & -\gamma_a & -\gamma_a & 0 & \varpi_h \end{pmatrix}.$$

The basic reproduction ratio \mathcal{R}_0 is then computed as the spectral radius of $F \cdot V^{-1}$. \square

Remark 1. *The last term in (9), that is, $\frac{\beta''(1 - \rho_1 - \rho_2)}{\delta_a}$, quantifies the number of susceptible that one asymptomatic individual infects through its infectious lifetime. This is an additional term to the basic reproduction number obtained in [6, 7], and it is responsible for a greater value to the basic reproduction number for the parameters of the new model considered in this paper.*

Next, we state and prove a theorem related to the stability of the disease free equilibrium point

$$DFE = (N, 0, 0, 0, 0, 0, 0, 0).$$

Theorem 4.3. *The disease free equilibrium DFE of system (6) is globally asymptotically stable whenever $\mathcal{R}_0 < 1$.*

Proof. To show global stability of DFE, we propose the following Lyapunov function:

$$V(t) = b_0 E(t) + b_1 I(t) + b_2 P(t) + b_3 A(t) + b_4 H(t),$$

where b_0, b_1, b_2, b_3 and b_4 are positive constants to be determined.

By linearity of the fractional operator ${}^c D^\alpha$, we have, for $\alpha_E = \alpha_I = \alpha_P = \alpha_A = \alpha_H = \alpha$, that

$${}^c D^\alpha V(t) = b_0 {}^c D^\alpha E(t) + b_1 {}^c D^\alpha I(t) + b_2 {}^c D^\alpha P(t) + b_3 {}^c D^\alpha A(t) + b_4 {}^c D^\alpha H(t),$$

and from (6) it follows that

$$\begin{aligned} {}^c D^\alpha V(t) &= b_0 \left(\beta \frac{I}{N} S + l\beta \frac{H}{N} S + \beta' \frac{P}{N} S + \beta'' \frac{A}{N} S - \kappa E \right) + b_1 (\kappa \rho_1 E - (\gamma_a + \gamma_i) I - \delta_i I) \\ &\quad + b_2 (\kappa \rho_2 E - (\gamma_a + \gamma_i) P - \delta_p P) + b_3 (\kappa(1 - \rho_1 - \rho_2) E - \delta_a A) \\ &\quad + b_4 (\gamma_a(I + P) - \gamma_r H - \delta_h H). \end{aligned}$$

Note that, because $0 \leq S \leq N$, we have

$$\begin{aligned} {}^c D^\alpha V(t) &\leq b_0 \left(\beta I + l\beta H + \beta' P + \beta'' A - \kappa E \right) + b_1 (\kappa \rho_1 E - \varpi_i I) \\ &\quad + b_2 (\kappa \rho_2 E - \varpi_p P) + b_3 (\kappa(1 - \rho_1 - \rho_2) E - \delta_a A) + b_4 (\gamma_a(I + P) - \varpi_h H). \end{aligned}$$

As a consequence, we obtain the following reduced inequality relationship:

$$\begin{aligned} {}^c D^\alpha V(t) &\leq (b_0 \beta + b_4 \gamma_a - b_1 \varpi_i) I + (b_0 \beta l - a_4 \varpi_h) H + (b_0 \beta' + b_4 \gamma - b_2 \varpi_p) P \\ &\quad + (b_0 \beta'' - b_3 \delta_a) A + \kappa (b_1 \rho_1 + b_2 \rho_2 + b_3 (1 - \rho_1 - \rho_2) - b_0) E. \end{aligned}$$

Thus, we fix the coefficients b_0, b_1, b_2, b_3, b_4 as follows:

$$\begin{aligned} b_0 &= \delta_a \varpi_i \varpi_p \varpi_h; & b_1 &= \left(\beta + \frac{\beta \gamma_a l}{\varpi_h} \right) \delta_a \varpi_h \varpi_p; & b_2 &= \left(\beta' + \frac{\beta \gamma_a l}{\varpi_h} \right) \delta_a \varpi_i \varpi_h; \\ & & b_3 &= \beta'' \varpi_i \varpi_h \varpi_p; & b_4 &= \beta l \delta_a \varpi_i \varpi_p. \end{aligned}$$

It is easy to check that our function V is continuous and positive definite for all $E(t) > 0$, $I(t) > 0$, $P(t) > 0$, $A(t) > 0$ and $H(t) > 0$. Moreover, we might also notice that

$$b_0 \beta + b_4 \gamma_a - b_1 \varpi_i = 0, \quad b_0 \beta l - a_4 \varpi_h = 0, \quad b_0 \beta' + b_4 \gamma - b_2 \varpi_p = 0, \quad b_0 \beta'' - b_3 \delta_a = 0,$$

and

$$\begin{aligned}
 b_1\rho_1 + b_2\rho_2 + b_3(1 - \rho_1 - \rho_2) - b_0 &= \beta\delta_a\rho_1\varpi_h\varpi_p + \beta\delta_a\rho_1\gamma_a l\varpi_p + \beta'\delta_a\rho_2\varpi_h\varpi_i + \beta\delta_a\rho_2\gamma_a l\varpi_i \\
 &\quad + \beta''(1 - \rho_1 - \rho_2)\varpi_i\varpi_h\varpi_p - \delta_a\varpi_i\varpi_p\varpi_h \\
 &= \left(\frac{\beta\delta_a\rho_1\varpi_h\varpi_p + \beta\delta_a\rho_1\gamma_a l\varpi_p + \beta'\delta_a\rho_2\varpi_h\varpi_i + \beta\delta_a\rho_2\gamma_a l\varpi_i + \beta''(1 - \rho_1 - \rho_2)\varpi_i\varpi_h\varpi_p}{\delta_a\varpi_i\varpi_p\varpi_h} - 1 \right) \\
 &\quad \times \delta_a\varpi_i\varpi_p\varpi_h \\
 &= \delta_a\varpi_i\varpi_p\varpi_h(R_0 - 1).
 \end{aligned}$$

Altogether, we obtain

$${}^c D^\alpha V(t) \leq \kappa \delta_a \varpi_i \varpi_p \varpi_h (R_0 - 1) E.$$

Therefore, ${}^c D^\alpha V(t) \leq 0$ whenever $R_0 < 1$. In addition, ${}^c D^\alpha V(t) = 0$ if, and only if, $E = I = P = H = 0$. Substituting $(E, I, P, H) = (0, 0, 0, 0)$ into system (6) leads to

$$S(t) = S(0), \quad A(t) = A(0), \quad R(t) = R(0), \quad F(t) = F(0).$$

Thus, we deduce that $A(0) = R(0) = F(0) = 0$ and $S(0) = N$, and the largest compact invariant set $\Gamma = \{(S, E, I, P, A, H, R, F) \in \mathbb{R}_+^8 : {}^c D^\alpha V(t) = 0\}$ becomes the disease free equilibrium point DFE . Finally, by the Lasalle invariance principle [17], we conclude that the disease free equilibrium DFE is globally asymptotically stable. \square

Global stability of the incommensurate fractional form of model (6) is confirmed through Ulam–Hyers stability [18], with recent COVID-19 model applications in [19]. We first discuss the conditions necessary to ensure the positiveness of the solutions.

Lemma 4.4. *The function $\mathbf{G}(t, \mathbf{X}(t))$ fulfills the Lipschitz conditions, specifically:*

$$(10) \quad \|\mathbf{G}(t, \mathbf{X}(t)) - \mathbf{G}(t, \mathbf{X}^*(t))\| \leq \Sigma \|\mathbf{X}(t) - \mathbf{X}^*(t)\|,$$

where

$$\begin{aligned}
 \mathbf{G}(t, \mathbf{X}(t)) &= (G_1(t, S(t)), G_2(t, E(t)), G_3(t, I(t)), G_4(t, P(t)), \\
 &\quad G_5(t, A(t)), G_6(t, H(t)), G_7(t, R(t)), G_8(t, F(t)))^\top
 \end{aligned}$$

is the vector of functions describing the system's dynamics (6), and

$$(11) \quad \Sigma = \max\{|\beta + l\beta + \beta' + \beta''|, |\kappa|, |\gamma_a + \gamma_i + \delta_i|, |\gamma_a + \gamma_i + \delta_p|, |\delta_a|, |\gamma_r + \delta_h|\}.$$

Proof. Summarizing that $S(t)$ and $S^*(t)$ are couple functions yields the following equality:

$$(12) \quad \|G_1(t, S(t)) - G_1(t, S^*(t))\| = \left\| \left(-\beta \frac{I}{N} - l\beta \frac{H}{N} - \beta' \frac{P}{N} - \beta'' \frac{A}{N} \right) (S(t) - S^*(t)) \right\|.$$

By defining

$$(13) \quad \Sigma_1 = |\beta + l\beta + \beta' + \beta''|,$$

we can infer the inequality

$$(14) \quad \|G_1(t, S(t)) - G_1(t, S^*(t))\| \leq \Sigma_1 \|S(t) - S^*(t)\|.$$

Proceeding similarly for the other functions yields

$$\begin{aligned}
(15) \quad & \|G_2(t, E(t)) - G_2(t, E^*(t))\| \leq \Sigma_2 \|E(t) - E^*(t)\| \\
& \|G_3(t, I(t)) - G_3(t, I^*(t))\| \leq \Sigma_3 \|I(t) - I^*(t)\| \\
& \|G_4(t, P(t)) - G_4(t, P^*(t))\| \leq \Sigma_4 \|P(t) - P^*(t)\| \\
& \|G_5(t, A(t)) - G_5(t, A^*(t))\| \leq \Sigma_5 \|A(t) - A^*(t)\| \\
& \|G_6(t, H(t)) - G_6(t, H^*(t))\| \leq \Sigma_6 \|H(t) - H^*(t)\| \\
& \|G_7(t, R(t)) - G_7(t, R^*(t))\| = 0 \\
& \|G_8(t, F(t)) - G_8(t, F^*(t))\| = 0,
\end{aligned}$$

with the Σ values specified as

$$\begin{aligned}
(16) \quad & \Sigma_2 = |\kappa|, \\
& \Sigma_3 = |\gamma_a + \gamma_i + \delta_i|, \\
& \Sigma_4 = |\gamma_a + \gamma_i + \delta_p|, \\
& \Sigma_5 = |\delta_a|, \\
& \Sigma_6 = |\gamma_r + \delta_h|.
\end{aligned}$$

This analysis, from equations (14) to (16), shows that all eight functions, F_i , meet the Lipschitz condition, validating their properties for the system (6). \square

Theorem 4.5. *Given the conditions of Lemma 4.4, if the inequality*

$$(17) \quad \Sigma \max_i \frac{T^{\alpha_i}}{\Gamma(\alpha_i + 1)} < 1, \quad i = S, E, I, P, A, H, R, F,$$

is satisfied, then the system (6) admits a unique, positive solution.

Proof. Using the integral form of the solution, we can derive the state variables expressed in terms of F_i as follows:

$$(18) \quad \begin{cases} S(t) = S(0) + \frac{1}{\Gamma(\alpha_S)} \int_0^t (t - \tau)^{\alpha_S - 1} G_1(\tau, S(\tau)) d\tau, \\ E(t) = E(0) + \frac{1}{\Gamma(\alpha_E)} \int_0^t (t - \tau)^{\alpha_E - 1} G_2(\tau, E(\tau)) d\tau, \\ I(t) = I(0) + \frac{1}{\Gamma(\alpha_I)} \int_0^t (t - \tau)^{\alpha_I - 1} G_3(\tau, I(\tau)) d\tau, \\ P(t) = P(0) + \frac{1}{\Gamma(\alpha_P)} \int_0^t (t - \tau)^{\alpha_P - 1} G_4(\tau, P(\tau)) d\tau, \\ A(t) = A(0) + \frac{1}{\Gamma(\alpha_A)} \int_0^t (t - \tau)^{\alpha_A - 1} G_5(\tau, A(\tau)) d\tau, \\ H(t) = H(0) + \frac{1}{\Gamma(\alpha_H)} \int_0^t (t - \tau)^{\alpha_H - 1} G_6(\tau, H(\tau)) d\tau, \\ R(t) = R(0) + \frac{1}{\Gamma(\alpha_R)} \int_0^t (t - \tau)^{\alpha_R - 1} G_7(\tau, R(\tau)) d\tau, \\ F(t) = F(0) + \frac{1}{\Gamma(\alpha_F)} \int_0^t (t - \tau)^{\alpha_F - 1} G_8(\tau, F(\tau)) d\tau. \end{cases}$$

By applying the Picard iteration [20] to Equation (18), we obtain the subsequent equations:

$$(19) \quad \begin{cases} S_{n+1}(t) = S(0) + \frac{1}{\Gamma(\alpha_S)} \int_0^t (t-\tau)^{\alpha_S-1} G_1(\tau, S(\tau)) d\tau, \\ E_{n+1}(t) = E(0) + \frac{1}{\Gamma(\alpha_E)} \int_0^t (t-\tau)^{\alpha_E-1} G_2(\tau, E(\tau)) d\tau, \\ I_{n+1}(t) = I(0) + \frac{1}{\Gamma(\alpha_I)} \int_0^t (t-\tau)^{\alpha_I-1} G_3(\tau, I(\tau)) d\tau, \\ P_{n+1}(t) = P(0) + \frac{1}{\Gamma(\alpha_P)} \int_0^t (t-\tau)^{\alpha_P-1} G_4(\tau, P(\tau)) d\tau, \\ A_{n+1}(t) = A(0) + \frac{1}{\Gamma(\alpha_A)} \int_0^t (t-\tau)^{\alpha_A-1} G_5(\tau, A(\tau)) d\tau, \\ H_{n+1}(t) = H(0) + \frac{1}{\Gamma(\alpha_H)} \int_0^t (t-\tau)^{\alpha_H-1} G_6(\tau, H(\tau)) d\tau, \\ R_{n+1}(t) = R(0) + \frac{1}{\Gamma(\alpha_R)} \int_0^t (t-\tau)^{\alpha_R-1} G_7(\tau, R(\tau)) d\tau, \\ F_{n+1}(t) = F(0) + \frac{1}{\Gamma(\alpha_F)} \int_0^t (t-\tau)^{\alpha_F-1} G_8(\tau, F(\tau)) d\tau. \end{cases}$$

Therefore, the system solution (6) can be expressed in the form

$$\mathbf{X}(t) = \mathcal{P}(\mathbf{X}(t)),$$

where $\mathbf{X}(t) = (S(t), E(t), I(t), P(t), A(t), H(t), R(t), F(t))^T$ is the state vector, and $\mathcal{P} : C([0, T], \mathbb{R}^8) \rightarrow C([0, T], \mathbb{R}^8)$ denotes the Picard operator. This operator is defined as follows:

$$(20) \quad \mathcal{P}(\mathbf{X}(t)) = \mathbf{X}(0) + \int_0^t \text{diag} \left(\frac{(t-\tau)^{\alpha_S-1}}{\Gamma(\alpha_S)}, \frac{(t-\tau)^{\alpha_E-1}}{\Gamma(\alpha_E)}, \frac{(t-\tau)^{\alpha_I-1}}{\Gamma(\alpha_I)}, \frac{(t-\tau)^{\alpha_P-1}}{\Gamma(\alpha_P)}, \right. \\ \left. \frac{(t-\tau)^{\alpha_A-1}}{\Gamma(\alpha_A)}, \frac{(t-\tau)^{\alpha_H-1}}{\Gamma(\alpha_H)}, \frac{(t-\tau)^{\alpha_R-1}}{\Gamma(\alpha_R)}, \frac{(t-\tau)^{\alpha_F-1}}{\Gamma(\alpha_F)} \right) \mathbf{G}(\tau, \mathbf{X}(\tau)) d\tau.$$

Simultaneously, we encounter the series of inequalities below:

(21)

$$\begin{aligned}
\|\mathcal{P}(\mathbf{X}(t)) - \mathcal{P}(\mathbf{X}^*(t))\| &= \left\| \int_0^t \text{diag} \left(\frac{(t-\tau)^{\alpha_S-1}}{\Gamma(\alpha_S)}, \frac{(t-\tau)^{\alpha_E-1}}{\Gamma(\alpha_E)}, \frac{(t-\tau)^{\alpha_I-1}}{\Gamma(\alpha_I)}, \right. \right. \\
&\quad \left. \left. \frac{(t-\tau)^{\alpha_P-1}}{\Gamma(\alpha_P)}, \frac{(t-\tau)^{\alpha_A-1}}{\Gamma(\alpha_A)}, \frac{(t-\tau)^{\alpha_H-1}}{\Gamma(\alpha_H)}, \frac{(t-\tau)^{\alpha_R-1}}{\Gamma(\alpha_R)}, \frac{(t-\tau)^{\alpha_F-1}}{\Gamma(\alpha_F)} \right) \right. \\
&\quad \left. \times (\mathbf{G}(\tau, \mathbf{X}(\tau)) - \mathbf{G}(\tau, \mathbf{X}^*(\tau))) d\tau \right\| \\
&\leq \left\| \int_0^t \text{diag} \left(\frac{(t-\tau)^{\alpha_S-1}}{\Gamma(\alpha_S)}, \frac{(t-\tau)^{\alpha_E-1}}{\Gamma(\alpha_E)}, \frac{(t-\tau)^{\alpha_I-1}}{\Gamma(\alpha_I)}, \right. \right. \\
&\quad \left. \left. \frac{(t-\tau)^{\alpha_P-1}}{\Gamma(\alpha_P)}, \frac{(t-\tau)^{\alpha_A-1}}{\Gamma(\alpha_A)}, \frac{(t-\tau)^{\alpha_H-1}}{\Gamma(\alpha_H)}, \frac{(t-\tau)^{\alpha_R-1}}{\Gamma(\alpha_R)}, \frac{(t-\tau)^{\alpha_F-1}}{\Gamma(\alpha_F)} \right) d\tau \right\| \\
&\quad \times \sup_{\tau \in [0, T]} \|\mathbf{G}(\tau, \mathbf{X}(\tau)) - \mathbf{G}(\tau, \mathbf{X}^*(\tau))\| \\
&\leq \max_{i=S, E, I, P, A, H, R, F} \int_0^t \frac{(t-\tau)^{\alpha_i-1}}{\Gamma(\alpha_i)} d\tau \sup_{\tau \in [0, T]} \|\mathbf{G}(\tau, \mathbf{X}(\tau)) - \mathbf{G}(\tau, \mathbf{X}^*(\tau))\| \\
&\leq \sum_{i=S, E, I, P, A, H, R, F} \max \frac{T^{\alpha_i}}{\Gamma(\alpha_i + 1)} \sup_{\tau \in [0, T]} \|\mathbf{X}(\tau) - \mathbf{X}^*(\tau)\|.
\end{aligned}$$

Given that $\sum \max_{i \in \{S, E, I, P, A, H, R, F\}} \frac{T^{\alpha_i}}{\Gamma(\alpha_i + 1)} < 1$ for $t \leq T$, the operator \mathcal{P} is established as a contraction. Consequently, system (6) is guaranteed to have a unique and positive solution, thereby completing the proof. \square

To provide a foundation for the subsequent discussion, we introduce the inequality expressed as follows:

$$(22) \quad |{}^C D_{0+}^\alpha \mathbf{X}(t) - \mathbf{G}(t, \mathbf{X}(t))| \leq \epsilon, \quad t \in [0, T],$$

in which $\alpha = \{\alpha_S, \alpha_E, \alpha_I, \alpha_P, \alpha_A, \alpha_H, \alpha_R, \alpha_F\}$ and $\epsilon = \{\epsilon_i | i = 1, \dots, 8\}$. We say a function $\bar{\mathbf{X}} \in \mathbb{R}_+^8$ is a solution of (22) if, and only if, there exists a perturbation $h \in \mathbb{R}_+^8$ satisfying

1. $|h(t)| \leq \epsilon$
2. ${}^C D_{0+}^\alpha \bar{\mathbf{X}}(t) = \mathbf{G}(t, \bar{\mathbf{X}}(t)) + h(t), \quad t \in [0, T]$.

Notably, by applying Equation (18) alongside property 2 mentioned above, straightforward simplification reveals that any function $\bar{\mathbf{X}} \in \mathbb{R}_+^8$ meeting the conditions of Equation (22) likewise fulfills the following associated integral inequality:

$$(23) \quad |\bar{\mathbf{X}}(t) - \bar{\mathbf{X}}(0) - \frac{1}{\Gamma(\alpha)} \int_0^t (t-\tau)^{\alpha-1} \mathbf{G}(\tau, \bar{\mathbf{X}}(\tau))| \leq \frac{T^\alpha}{\Gamma(\alpha+1)} \epsilon.$$

Let $\mathfrak{G} = C([0, T]; \mathbb{R})$ denote the Banach space of all continuous functions from $[0, T]$ to \mathbb{R} equipped with the norm $\|\mathbf{X}\|_{\mathfrak{G}} = \sup_{t \in [0, T]} \{|\mathbf{X}|\}$, where $|\mathbf{X}| = |S(t)| + |E(t)| + |I_A(t)| + |I_S(t)| + |R(t)| + |D(t)| + |W(t)|$.

The fractional order model (6) achieves Ulam–Hyers stability if there are some $\Sigma > 0$ ensuring that, for any given $\bar{\epsilon} = \mathbb{R}_+$, and for every solution $\bar{\mathbf{X}}$ meeting the conditions of (22), a corresponding solution \mathbf{X} to (6) can be found where

$$(24) \quad \|\bar{\mathbf{X}}(t) - \mathbf{X}(t)\|_{\mathfrak{G}} \leq \Sigma \bar{\epsilon}, \quad t \in [0, T].$$

Moreover, this model is deemed to be generalized Ulam–Hyers stable if a continuous function $\Sigma_G : \mathbb{R}_+ \rightarrow \mathbb{R}_+$ exists, satisfying $\Sigma_G(0) = 0$. This condition requires that, for any solution $\bar{\mathbf{X}}$ of (22), there must be a corresponding solution \mathbf{X} of (6) for which

$$(25) \quad \|\bar{\mathbf{X}}(t) - \mathbf{X}(t)\|_{\mathfrak{G}} \leq \Sigma_G \bar{\epsilon}, \quad t \in [0, T].$$

We proceed to detail the stability results for the fractional order model.

Theorem 4.6. *Assuming the conditions and conclusions of Lemma 4.4 and Theorem 4.5 are satisfied, i.e. $\Sigma \max_i \frac{T^{\alpha_i}}{\Gamma(\alpha_i + 1)} < 1$, it follows that the model specified in (6) exhibits generalized Ulam–Hyers stability.*

Proof. Given that \mathbf{X} is a unique solution to (6) confirmed by Lemma 4.4 and Theorem 4.5, and $\bar{\mathbf{X}}$ meets the criteria of (22), reference to equations (18) and (23) leads us to conclude that for any $\epsilon \in \mathbb{R}_+^8$ and $t \in [0, T]$, the following relationship holds:

$$(26) \quad \begin{aligned} \|\bar{\mathbf{X}} - \mathbf{X}\|_{\mathfrak{G}} &= \sup_{t \in [0, T]} |\bar{\mathbf{X}} - \mathbf{X}| \\ &= \sup_{t \in [0, T]} \left| \bar{\mathbf{X}} - \mathbf{X}_0 - \frac{1}{\Gamma(\alpha)} \int_0^t (t - \tau)^{\alpha-1} \mathbf{G}(t, \mathbf{X}(\tau)) d\tau \right| \\ &\leq \sup_{t \in [0, T]} \left| \bar{\mathbf{X}}(t) - \bar{\mathbf{X}}_0 - \frac{1}{\Gamma(\alpha)} \int_0^t (t - \tau)^{\alpha-1} \mathbf{G}(t, \bar{\mathbf{X}}(\tau)) d\tau \right| \\ &\quad + \sup_{t \in [0, T]} \frac{1}{\Gamma(\alpha)} \int_0^t (t - \tau)^{\alpha-1} |\mathbf{G}(t, \bar{\mathbf{X}}(\tau)) - \mathbf{G}(t, \mathbf{X}(\tau))| d\tau \\ &\leq \frac{\epsilon T^\alpha}{\Gamma(\alpha + 1)} + \frac{\Sigma}{\Gamma(\alpha)} \sup_{t \in [0, T]} \int_0^t (t - \tau)^{\alpha-1} |\bar{\mathbf{X}}(\tau) - \mathbf{X}(\tau)| d\tau \\ &\leq \max_{i=S, E, I, P, A, H, R, F} \left(\frac{\bar{\epsilon} T^{\alpha_i}}{\Gamma(\alpha_i + 1)} + \frac{\Sigma T^{\alpha_i}}{\Gamma(\alpha_i + 1)} \|\bar{\mathbf{X}}(\tau) - \mathbf{X}(\tau)\|_{\mathfrak{G}} \right), \end{aligned}$$

where, $\bar{\epsilon} = \max_i \epsilon_i$. From this, we derive that $\|\bar{\mathbf{X}} - \mathbf{X}\|_{\mathfrak{G}} \leq \Sigma_G \bar{\epsilon}$, with Σ_G defined as

$$\Sigma_G = \max_{i=S, E, I, P, A, H, R, F} \frac{T^{\alpha_i}}{\Gamma(\alpha_i + 1) - T^{\alpha_i} \Sigma}.$$

The proof is complete. □

5. NUMERICAL RESULTS

This section presents the efficiency of our proposed model in simulating the dynamics of COVID-19 transmission, which integrates the variables of asymptomatic and super-spreader individuals. The model is calibrated using real-world data of Portugal obtained from the Center for Systems Science and Engineering (CSSE) at Johns Hopkins University [21]. The initial conditions for the model are described as follows:

$$(27) \quad \begin{aligned} N_0 &= 10280000/1363, \\ S_0 &= N_0 - 5, \quad E_0 = 0, \quad I_0 = 4, \quad P_0 = 1, \quad A_0 = 0, \quad H_0 = 0, \quad R_0 = 0, \quad F_0 = 0, \end{aligned}$$

while Table 1 provides the values of the model parameters used in the analysis.

We evaluate the performance of the proposed model (6) in the context of the absence of super-spreaders or asymptomatic individuals. Our model incorporates additional coefficients to account for the contribution of asymptomatic and super-spreader individuals to the transmission of the disease. Thus, we consider six variations of our proposed model (6), each with different constraints and orders of derivatives, to compare their performance in modelling. The first three models are named M1, M2, and M3, and they utilize integer-order derivatives.

Model M1 lacks the influence of super-spreader individuals P and their related coefficients, β' , ρ_2 , and δ_p . Model M2 excludes asymptomatic individuals and their coefficients, meaning compartment A and its related coefficients β'' and δ_a are set to zero. In this case, instead of using ρ_2 , we simply use $1 - \rho_1$, thus eliminating the need for the parameter ρ_2 . Model M3 represents our proposed model with integer-order derivatives.

Furthermore, we compare the fractional-order forms of the models, denoted as FM1, FM2, and FM3, respectively. The following box summarizes all the models together.

Summary of the Models

Integer-Order Models

- M1** : Model (6) lacking super-spreader individuals ($P = 0, \beta', \rho_2, \delta_p = 0$)
- M2** : Model (6) lacking asymptomatic individuals ($A = 0, \beta'', \delta_a = 0, \rho_2 = 1 - \rho_1$)
- M3** : Model (6) with super-spreader and asymptomatic individuals

Fractional-Order Models

- FM1** : Fractional-order version of M1
- FM2** : Fractional-order version of M2
- FM3** : Fractional-order version of M3

We obtain the values of parameters, including $\beta, \beta', \beta'', \rho_1, \rho_2, \delta_p$, and δ_a , by fitting the models to the data. In the case of fractional models (FM1, FM2, and FM3), we optimize the values of order derivatives and parameters to achieve the best possible fit. The resulting fitted values and their root mean square deviation (RMSD) for all models can be found

TABLE 2. Optimized values of parameters for models M1, M2, and M3, with integer orders and the order derivatives, denoted as $\alpha_{S,E,I,P,A,H,R,F}$ for models FM1, FM2, and FM3, obtained by fitting COVID-19 data from Portugal and evaluated based on their root mean square deviation (RMSD) errors.

Parameters	M1	FM1	M2	FM2	M3	FM3
β	3.3687	3.4956	3.1300	3.5122	3.1221	2.9763
β'	-	-	7.9889	7.7403	5.0792	7.8959
β''	4.9091	5.0111	-	-	4.6831	2.7722
ρ_1	0.7010	0.6002	0.8760	0.8311	0.5990	0.5273
ρ_2	-	-	-	-	0.1500	0.2509
δ_p	-	-	0.0197	0.0400	0.0010	0.0017
δ_a	0.0055	0.0061	-	-	0.0097	0.0204
α_S	-	0.9035	-	1.0000	-	0.9786
α_E	-	1.0000	-	0.9776	-	1.0000
α_I	-	1.0000	-	0.8932	-	1.0000
α_P	-	0.8500	-	1.0000	-	1.0000
α_A	-	1.0000	-	0.8500	-	1.0000
α_H	-	1.0000	-	1.0000	-	1.0000
α_F	-	0.8998	-	1.0000	-	0.9399
RMSD	123.3005	107.4498	116.4057	109.8153	108.2076	99.3987

in Table 2, such that $\text{RMSD}(x, \hat{x}) = \sqrt{\frac{1}{n} \sum_{t=1}^n (x_t - \hat{x}_t)^2}$, where, n is the number of data points, x approximated values, and \hat{x} real values.

Figure 1 illustrates the models' effectiveness in fitting daily new confirmed cases and cumulative death cases. The comparison shows that Model M1, with an error of 123.30, performs worse than the other models. However, the fractional form of this model, FM1, improves accuracy, reducing the error to 107.45.

Model M2 shows better performance with an error of 116.41. The fractional form, FM2, further improves the fit, achieving an error of 109.81. This improvement is less significant than that seen in FM1.

Our proposed model (6) with integer-order derivatives, M3, which includes both asymptomatic and super-spreader compartments, outperforms M1 and M2, with an error of 108.21. The fractional-order version, FM3, further enhances accuracy, reducing the error to 99.40, making it the best-performing model among all.

Figure 2 presents a comprehensive comparison of the individual dynamics obtained from simulations of the six studied models. The simulations were conducted using the fitted orders of derivatives and parameters, as outlined in Tables 1 and 2. The figure visually illustrates the distinct behaviours of the models for different individual cases, highlighting the impact of the chosen order derivatives and parameters on the dynamics of the disease spread.

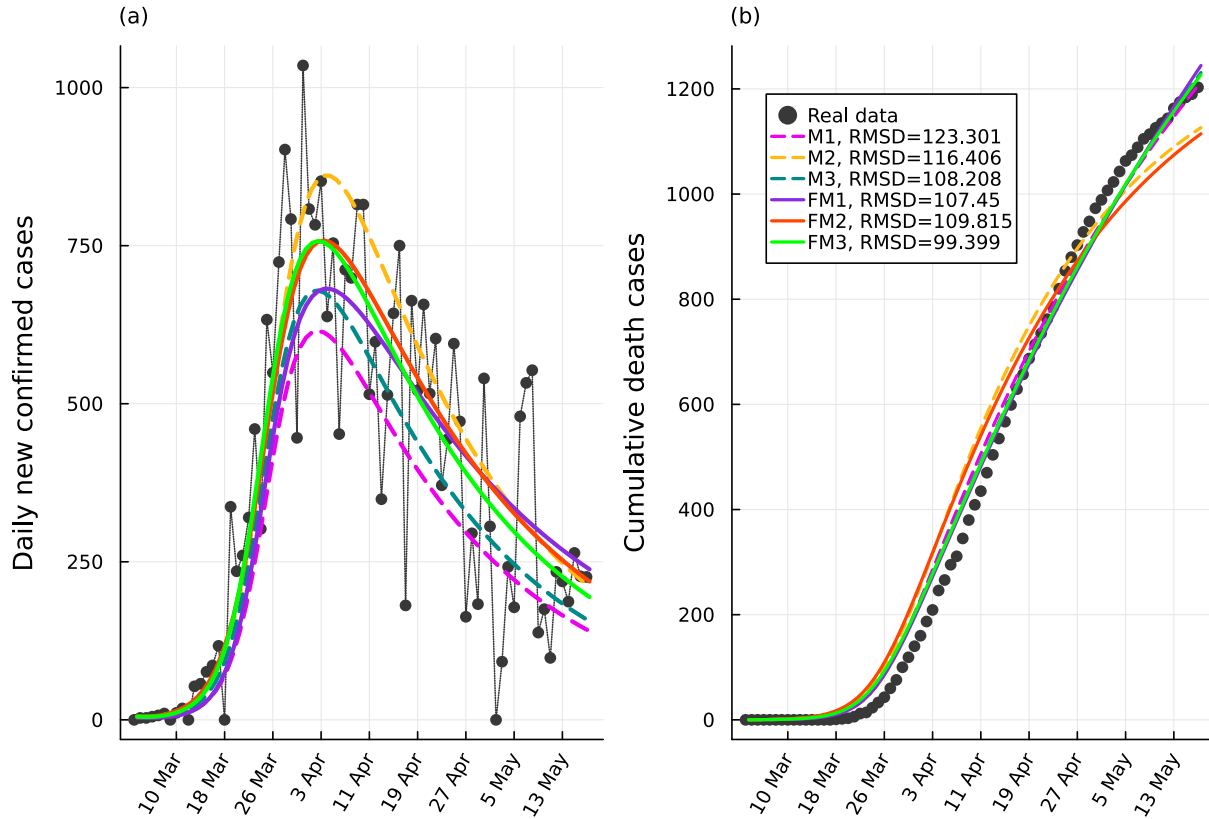


FIGURE 1. Illustration of the accuracy of the studied models in fitting (a) daily new confirmed cases and (b) cumulative death cases, as retrieved from CSSE [21]. The estimation of variables $I + P + H$ and F is shown. Data points are represented by black circles. Errors are evaluated using the root mean square deviation (RMSD). Model M1, which lacks super-spreaders and uses integer orders, is shown to have an inferior performance with an error of 123.30. The fractional version of this model, FM1 (solid purple line), improves accuracy significantly, reducing the error to 107.45. Model M2, which lacks asymptomatic individuals (dashed orange line), performs better than M1 with an error of 116.41. However, its fractional version, FM2 (solid red line), shows a smaller improvement compared to FM1, with an error of 109.81. Our proposed model (6) with integer orders, M3 (dashed green line), which includes both super-spreader and asymptomatic compartments, performs better than both M1 and M2, with an error of 108.21. The fractional version of this model, FM3 (solid green line), shows the best performance, reducing the error to 99.40.

5.1. Sensitivity Analysis of the Basic Reproduction Number. This section aims to elucidate the impact of varying variables on the propagation of infectious illnesses. By evaluating the sensitivity of \mathcal{R}_0 to different parameters, such as social distancing measures,

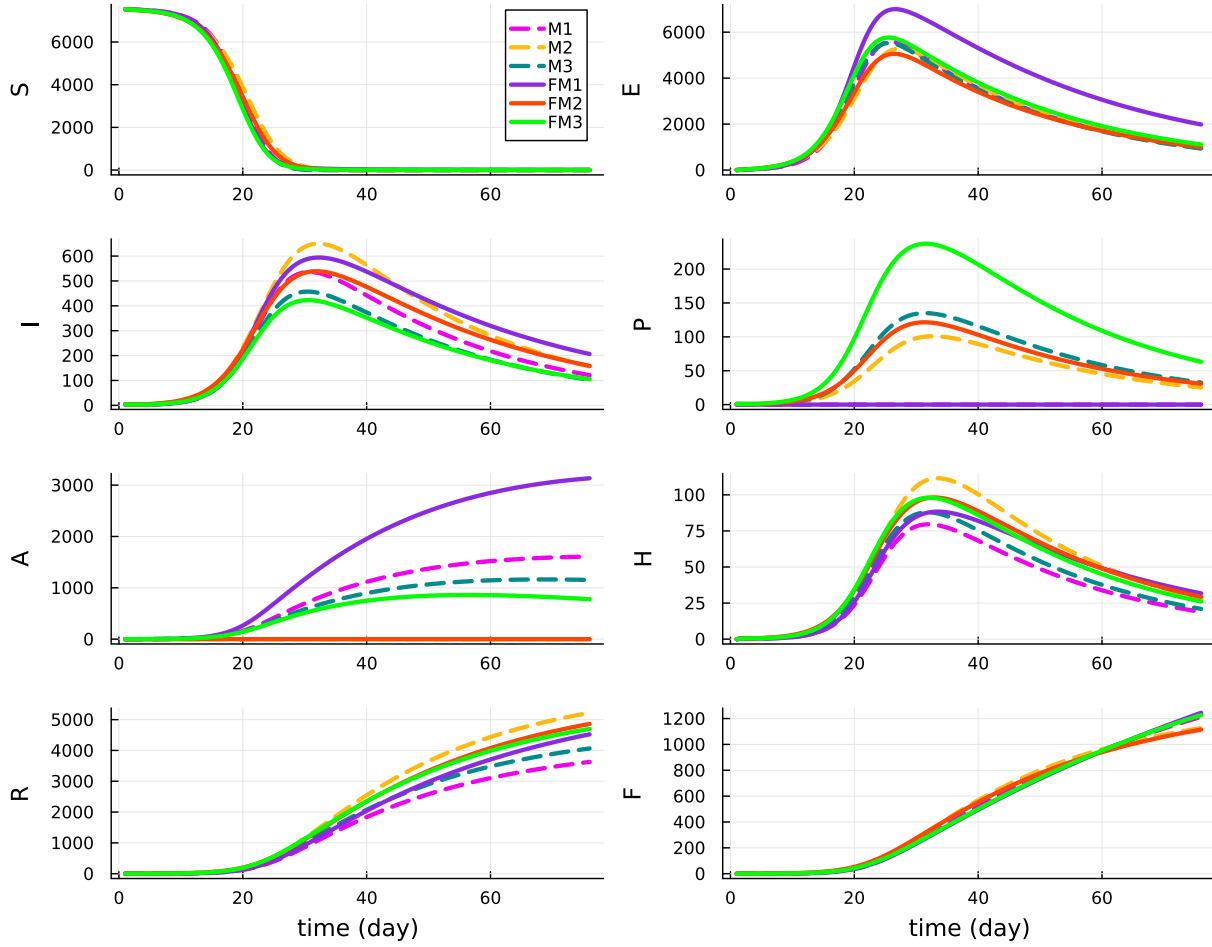


FIGURE 2. Comparison of individual dynamics from simulations of six studied models: Model M1 excludes super-spreaders (with parameters β' , ρ_2 , $\delta_p = 0$), and uses integer-order derivatives. Model M2 excludes asymptomatic individuals (with parameters β'' , $\delta_a = 0$, $\rho_2 = 1 - \rho_1$), and also uses integer-order derivatives. Model M3 is the proposed model (6) that includes both super-spreader and asymptomatic compartments, using integer-order derivatives. The fractional-order models are as follows: FM1 is the fractional-order version of M1, FM2 is the fractional-order version of M2, and FM3 is the fractional-order version of M3. The values for parameters and orders of the derivatives used in simulations are provided in Tables 1 and 2.

policy-makers can make informed decisions about public health interventions. Additionally, this approach enables the identification of parameters with the greatest impact on disease spread. To determine the effects of minor adjustments in parameter \mathcal{P} on the basic reproduction number \mathcal{R}_0 , we introduce the forward normalized sensitivity index of \mathcal{R}_0 for

\mathcal{P} , which can be expressed as follows:

$$\mathcal{S}_{\mathcal{P}}^{\mathcal{R}_0} = \frac{\partial \mathcal{R}_0}{\partial \mathcal{P}} \frac{\mathcal{P}}{\mathcal{R}_0}.$$

We have computed the sensitivity indices for \mathcal{R}_0 , associated with the estimated parameters for models, and their corresponding values are presented in Table 3.

TABLE 3. Sensitivity index of \mathcal{R}_0 across all parameters ($\mathcal{S}_{\mathcal{P}}^{\mathcal{R}_0}$) and models.

Parameters	M1	FM1	M2	FM2	M3	FM3
β	0.0435	0.0324	0.7601	0.7380	0.0766	0.1843
β'	-	-	0.2399	0.2620	0.0290	0.2055
β''	0.9565	0.9676	-	-	0.8944	0.6102
l	0.0084	0.0063	0.1651	0.1656	0.0182	0.0506
ρ_1	-2.1883	-1.4190	-1.1173	-0.7190	-2.0742	-1.2845
ρ_2	-	-	-	-	-0.5034	-0.4660
γ_a	-0.0161	-0.0120	-0.4127	-0.3990	-0.0450	-0.1937
γ_i	-0.0098	-0.0073	-0.2326	-0.2272	-0.0255	-0.0986
γ_r	-0.0083	-0.0062	-0.1627	-0.1632	-0.0180	-0.0499
δ_i	-0.0078	-0.0058	-0.1317	-0.1267	-0.0129	-0.0296
δ_p	-	-	-0.0231	-0.0477	-0.0002	-0.0019
δ_h	-3.14e-5	-2.34e-5	-0.0006	-0.0006	-6.81e-5	-0.0002
δ_a	-0.3415	-0.3674	-	-	-0.4403	-0.4096

It is clear that if \mathcal{R}_0 increases concerning \mathcal{P} , then the sensitivity index of $\mathcal{S}_{\mathcal{P}}^{\mathcal{R}_0}$ is positive; and if \mathcal{R}_0 decreases concerning \mathcal{P} , then the sensitivity index is negative. To elaborate further, a sensitivity index of $\mathcal{S}_{\beta''}^{\mathcal{R}_0} = 0.9565$ implies that an increase of 1% in β'' , keeping all other parameters constant, will lead to a 0.9565% increase in \mathcal{R}_0 . Similarly, $\mathcal{S}_{\rho_1}^{\mathcal{R}_0} = -2.1883$ means that increasing the parameter ρ_1 by 1%, while holding all other parameters constant, will cause a decrease in the value of \mathcal{R}_0 by 2.1883%.

According to Table 3, the most influential parameter for models M1, FM1, M3, and FM3, contributing to the increase in the value of \mathcal{R}_0 , is β'' , whereas it is β in models M2 and FM2. The most influential parameter contributing to its reduction is ρ_1 for all models.

5.2. Numerical methods and implementation. We conducted all the numerical analyses using the programming language `Julia` and the high-performance computing system `PUHTI` at the Finnish IT Center for Science (CSC). To solve fractional differential equations, we made use of the `FdeSolver.jl` package (v 1.0.7) that applies predictor-corrector algorithms and product-integration rules [22]. Parameter estimation was accomplished through Bayesian inference and Hamiltonian Monte Carlo (HMC) using `Turing.jl`, while ODEs were solved with `DifferentialEquations.jl`. The order of derivatives was optimized through the function (L)BFGS, based on the (Limited-memory) Broyden–Fletcher–Goldfarb–Shanno algorithm from the `Optim.jl` package and `FdeSolver.jl`.

6. CONCLUSION

Our study presents an innovative approach to modelling COVID-19 transmission dynamics by integrating asymptomatic and super-spreader individuals into a single model using fractional calculus. Furthermore, we have conducted a qualitative analysis of our proposed model, which includes determining the basic reproduction number and analysing the disease-free equilibrium. Our findings emphasize the benefits of incommensurate fractional order derivatives, such as increased flexibility in capturing disease dynamics and refined memory effects in the transmission process. By fitting the proposed model with real data from Portugal and comparing it with existing models, we demonstrate that including supplementary coefficients and fractional derivatives enhances the model's goodness of fit. Sensitivity analysis further provides valuable insights for policy-makers in designing effective strategies to mitigate the spread of COVID-19. Overall, our study contributes to the literature on fractional modelling of COVID-19 transmission and has potential implications for understanding and controlling the spread of infectious diseases.

STATEMENTS AND DECLARATIONS

Competing Interests. The authors declare no conflicts of interest.

Data and Code Availability. All computational results for this paper are available on GitHub, and accessible via the permanent Zenodo DOI: <https://doi.org/10.5281/zenodo.14607808>.

Funding. This study has been supported by the Academy of Finland (330887 to MK, LL) and the UTUGS graduate school of the University of Turku (to MK). FN is supported by the Bulgarian Ministry of Education and Science, Scientific Programme “Enhancing the Research Capacity in Mathematical Sciences (PIKOM)”, Contract No. DO1–67/05.05.2022. DFMT is supported by FCT (Fundação para a Ciência e a Tecnologia) through CIDMA projects UIDB/04106/2020 (<https://doi.org/10.54499/UIDB/04106/2020>) and UIDP/04106/2020 (<https://doi.org/10.54499/UIDP/04106/2020>), and the CoSysM3 project 2022.03091.PTDC (<https://doi.org/10.54499/2022.03091.PTDC>).

Acknowledgements. The authors wish to acknowledge CSC-IT Center for Science, Finland, for computational resources and high-speed networking.

REFERENCES

- [1] P. Agarwal, J. J. Nieto, M. Ruzhansky and D. F. M. Torres, Analysis of Infectious Disease Problems (Covid-19) and Their Global Impact, Infosys Science Foundation Series in Mathematical Sciences, Springer, Singapore, 2021.
- [2] P. Agarwal, J. J. Nieto and D. F. M. Torres. Mathematical Analysis of Infectious Diseases, Academic Press, London, UK, 2022.
- [3] C. J. R. Illingworth, W. L. Hamilton, B. Warne, M. Routledge, A. Popay, C. Jackson, T. Fieldman, L. W. Meredith, C. J. Houldcroft, M. Hosmillo, et al. Superspreaders drive the largest outbreaks of hospital onset COVID-19 infections. *eLife*, 10:e67308, 2021.
- [4] M. Aguiar, E.M. Ortuondo, J. Bidaurrazaga Van-Dierdonck, et al. Modelling COVID-19 in the Basque Country from introduction to control measure response. *Sci. Rep.* 10:17306, 2020.

- [5] H. Zine, A. Boukhouima, E. M. Lotfi, M. Mahrouf, D. F. M. Torres, N. Yousfi. A stochastic time-delayed model for the effectiveness of Moroccan COVID-19 deconfinement strategy, *Math. Model. Nat. Phenom.* 15:50, 2020. [arXiv:2010.16265](#)
- [6] F. Ndaïrou, I. Area, G. Bader, J. J. Nieto, D. F. M. Torres. Corrigendum to 'Mathematical modeling of COVID-19 transmission dynamics with a case study of Wuhan' [*Chaos Solitons Fractals* 135 (2020), 109846], *Chaos Solitons & Fractals* 141 (2020): 110311.
- [7] F. Ndaïrou, I. Area, J. J. Nieto, D. F. M. Torres. Mathematical modeling of COVID-19 transmission dynamics with a case study of Wuhan. *Chaos Solitons & Fractals* 135 (2020): 109846. [arXiv:2004.10885](#)
- [8] F. Ndaïrou, D. F. M. Torres. Mathematical Analysis of a Fractional COVID-19 Model Applied to Wuhan, Spain and Portugal. *Axioms* 2021, 10:135. [arXiv:2106.15407](#)
- [9] M. Saeedian, M. Khalighi, N. Azimi-Tafreshi, G. R. Jafari, M. Ausloos. Memory effects on epidemic evolution: The susceptible-infected-recovered epidemic model. *Phys Rev E* 95(2):022409, 2017.
- [10] H. Jahanshahi, J.M. Munoz-Pacheco, S. Bekiros, N.D. Alotaibi A fractional-order SIRD model with time-dependent memory indexes for encompassing the multi-fractional characteristics of the COVID-19. *Chaos, Solitons & Fractals* 143 (2021): 110632.
- [11] H. Ye, J. Gao, Y. Ding. A generalized Gronwall inequality and its application to a fractional differential equation. *J. Math. Anal. Appl.* 328:1075–1081, 2007.
- [12] W. Lin. Global existence theory and chaos control of fractional differential equations. *J. Math. Anal. Appl.* 332:709–726, 2007.
- [13] M. A. Johansson, T. M. Quandelacy, S. Kada, et al. SARS-CoV-2 Transmission From People Without COVID-19 Symptoms. *JAMA Netw Open.* 2021, 4(1):e2035057.
- [14] D. Majra, J. Benson, J. Pitts, J. Stebbing. SARS-CoV-2 (COVID-19) superspreader events. *J Infect.* 2021, 82(1):36–40.
- [15] K. Dietz. Overall Population Patterns in the Transmission Cycle of Infectious Disease Agents (1982) In: Anderson, R.M., May, R.M. (eds) *Population Biology of Infectious Diseases*. Dahlem Workshop Reports, vol 25. Springer, Berlin, Heidelberg.
- [16] O. Diekmann, J. A Heesterbeek, M. G. Roberts. The construction of next-generation matrices for compartmental epidemic models. *J. R. Soc. Interface* 7(47):873–885, 2010.
- [17] J. P. LaSalle. Stability theory for ordinary differential equations, *Journal of Differential Equations* 4(1) (1968): 57–65.
- [18] S.-M. Jung. *Hyers-Ulam-Rassias stability of functional equations in nonlinear analysis*. Springer Science & Business Media, volume 48, 2011.
- [19] I. A. Baba, D. Baleanu. Awareness as the Most Effective Measure to Mitigate the Spread of COVID-19 in Nigeria. *Computers, Materials & Continua*, 65(3):1945–1957, 2020.
- [20] A. Boudaoui, Y. El hadj Moussa, Z. Hammouch, S. Ullah. A fractional-order model describing the dynamics of the novel coronavirus (COVID-19) with nonsingular kernel. *Chaos, Solitons & Fractals*, 146:110859, 2021.
- [21] E. Dong, H. Du, L. Gardner. An interactive web-based dashboard to track COVID-19 in real time. *The Lancet infectious diseases* 20(5): 533–534, 2020.
- [22] M. Khalighi, G. Benedetti, L. Lahti. Algorithm 1047: FdeSolver, a Julia Package for Solving Fractional Differential Equations. *ACM Transactions on Mathematical Software* 50(3), Art. 22, 1–23, 2024. [arXiv:2212.12550](#)

(M. Khalighi) DEPARTMENT OF COMPUTING, UNIVERSITY OF TURKU, TURKU, FINLAND
Email address: moein.khalighi@utu.fi

(L. Lahti) DEPARTMENT OF COMPUTING, UNIVERSITY OF TURKU, TURKU, FINLAND
Email address: leo.lahti@utu.fi

(F. Ndairou) INSTITUTE OF MATHEMATICS AND INFORMATICS, BULGARIAN ACADEMY OF SCIENCES,
SOFIA 1113, BULGARIA
Email address: faical@math.bas.bg

(P. Rashkov) INSTITUTE OF MATHEMATICS AND INFORMATICS, BULGARIAN ACADEMY OF SCIENCES,
SOFIA 1113, BULGARIA
Email address: p.rashkov@math.bas.bg

(D. F. M. Torres) CENTER FOR RESEARCH AND DEVELOPMENT IN MATHEMATICS AND APPLICATIONS
(CIDMA), DEPARTMENT OF MATHEMATICS, UNIVERSITY OF AVEIRO, AVEIRO 3810–193, PORTUGAL
Email address: delfim@ua.pt